Two-ball problem revisited: Limitations of event-driven modeling

Patric Müller* and Thorsten Pöschel
Institute for Multiscale Simulation, Universität Erlangen-Nürnberg, Nägelsbachstraße 49b, D-91052 Erlangen, Germany
(Received 13 January 2011; published 25 April 2011)

The main precondition of simulating systems of hard particles by means of event-driven modeling is the assumption of instantaneous collisions. The aim of this paper is to quantify the deviation of event-driven modeling from the solution of Newton's equation of motion using a paradigmatic example: If a tennis ball is held above a basketball with their centers vertically aligned, and the balls are released to collide with the floor, the tennis ball may rebound at a surprisingly high speed. We show in this article that the simple textbook explanation of this effect is an oversimplification, even for the limit of perfectly elastic particles. Instead, there may occur a rather complex scenario including multiple collisions which may lead to a very different final velocity as compared with the velocity resulting from the oversimplified model.

DOI: 10.1103/PhysRevE.83.041304 PACS number(s): 45.70.−n, 45.50.Tn

I. INTRODUCTION

Consider a set of two balls made of the same viscoelastic material whose centers are vertically aligned at positions z_1 and z_2 as sketched in Fig. 1. Let R_1 and R_2 be the radii of the particles and Δh their initial vertical spacing. At time $t = 0$ we release the particles to collide with the floor. The question for the maximum height reached by the upper sphere after the collision is then a common textbook problem. The textbook solution is based on the assumption that the collisions of the lower particle with the floor and the subsequent collision of the lower particle with the upper one are separate two-body interactions which may be treated independently; that is, one disregards the duration of the collisions. Whether this assumption is justified depends, of course, on the initial conditions, the particle sizes, and the material parameters.

The experimental investigation of the described problem is tricky as even a small deviation from the vertical alignment of the initial positions of the spheres leads to considerable postcollisional velocities in horizontal direction, in particular, if more than two balls are involved. Simple but effective techniques were introduced [1,2], which allow for experiments with chains of up to about 7 aligned balls.

In this paper we will show that although the problem looks simple, there may emerge rather complex behavior including multiple collisions. The simple solution mentioned above is, thus, only a special case of a more general solution.

II. INDEPENDENT-COLLISIONS MODEL

A. Collision scenario

To introduce our notation and for later reference let us first reproduce the solution for the independent-collisions model (ICM); that is, the final velocity of the upper ball is the result of (a) the inelastic collision of the lower ball with the floor and (b) the inelastic collision of the lower ball with the upper ball. Note that here and in the following we restrict ourselves to the situation where $m_1 > m_2$. For the opposite case, $m_1 < m_2$, it may be shown that the sketched sequence of collisions fails, even under the assumption of perfectly elastic collisions [1,3].

Inelasticity of the balls is described by the coefficient of restitution which relates the precollisional relative velocity $v_{ij} = v_i - v_j$ of colliding particles i and j to the postcollisional one, $v'_{ij} = v'_i - v'_j$,

$$\varepsilon = -v'_{ij}/v_{ij}. \tag{1}$$

The lower sphere (m_1) reaches the floor at time $t_{10} = \sqrt{\frac{2}{g}(z_1^{(0)} - R_1)}$ at the velocity $v_{10} = -\sqrt{2g(z_1^{(0)} - R_1)}$ from where it is reflected with $v'_{10} = -\varepsilon v_{10}$. The first index always denotes the considered particle and the second its collision partner. Index 0 stands for the floor, 1 for the lower sphere, and 2 for the upper sphere. Upper index $^{(0)}$ stands for initial values. Postcollisional values are marked by primes. The particles collide then at $t_{12} = t_{10} - \frac{\Delta h}{v_{10}(1+\varepsilon)} \equiv t_{10} + \Delta t$ whereby the upper sphere is located at position $z_{21} = z'_{21} = -\frac{1}{2}gt_{12}^2 + z_2^{(0)}$ with the initial height $z_2^{(0)} = z_1^{(0)} + R_1 + R_2 + \Delta h$. At t_{12} the lower particle has the velocity $v_{12} = -g\Delta t + v'_{10}$ and the upper $v_{21} = -gt_{12}$. Employing the collision rule, Eq. (1), and conservation of momentum, we obtain the final velocities

$$v'_2 = \frac{m_2 v_{21} + m_1[v_{12} + \varepsilon(v_{12} - v_{21})]}{m_1 + m_2}, \tag{2}$$

$$v'_1 = \frac{m_1 v_{12} + m_2[v_{21} + \varepsilon(v_{21} - v_{12})]}{m_1 + m_2} \tag{3}$$

and the relative velocity

$$v'_r = v'_2 - v'_1. \tag{4}$$

In the case of elastic ($\varepsilon = 1$) and instantaneous ($\Delta h \to 0$) collisions we find

$$v'_2 = -v_{10}\frac{3-\mu}{1+\mu} \quad \text{with} \quad \mu = \frac{m_2}{m_1}, \tag{5}$$

$$v'_1 = -v_{10}\frac{1-3\mu}{1+\mu}. \tag{6}$$

For $\mu = \frac{1}{3}$ the lower sphere loses all its kinetic energy ($v'_1 = 0$) and the upper sphere rebounds with twice its initial velocity. In the limit $\mu \to 0$ we recover the well known textbook result

*patric.mueller@cbi.uni-erlangen.de

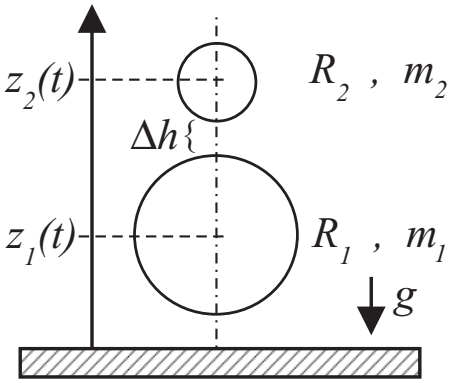

FIG. 1. Sketch of the problem.

$v_2' = -3v_{10}$; that is, the upper ball rises to about nine times its initial drop height [$z_2^{\max} = 9z_2^{(0)} - 8(2R_1 + R_2)$].

The system of bouncing balls can be exhaustively described also for more than two spheres [4], provided the collisions are considered as isolated events, that is, only two-particle interactions are taken into account.

B. Coefficient of restitution resulting from the solution of Newton's equation

The contact of viscoelastic spheres is described by the (modified) Hertz contact law [5]. In this article we will use a simplified force law since it allows for an exhaustive analytical solution of the problem. To justify this approximation, we will show later by means of numerical simulations that the more correct Hertz contact force leads to qualitatively identical results, see Appendix B.

We describe the contact of dissipatively interacting particles i and j by

$$F(\xi_{ij},\dot{\xi}_{ij}) = \min[0, -k\xi_{ij} - \gamma\dot{\xi}_{ij}] \tag{7}$$

as a function of the mutual compression

$$\xi_{ij}(t) = \max[0, R_i + R_j - |\vec{r}_i(t) - \vec{r}_j(t)|] \tag{8}$$

and the compression rate $\dot{\xi}_{ij} = d\xi_{ij}(t)/dt$, where R_i is the radius of particle i and $\vec{r}_i(t)$ is its position at time t. The expression in square brackets in Eq. (7) may become positive during the expansion phase; that is, the (positive) dissipative force may overcompensate the (negative) elastic force which would lead to a resulting erroneous attractive force, see, e.g., [6]. Therefore, the min[$\cdots$] function is applied to take into account that the interaction force is always repulsive (negative).

Consider an isolated pair of colliding particles i and j approaching one another at impact rate $v = \dot{\xi}(t = 0)$ at $t = 0$. Using the force, Eq. (7), we obtain the relative velocity after a collision by solving Newton's equation of motion,

$$m_{ij}^{\text{eff}}\ddot{\xi}_{ij} = F(\dot{\xi}_{ij},\xi_{ij}), \tag{9}$$

with the effective mass $m_{ij}^{\text{eff}} = m_i m_j/(m_i + m_j)$ and initial conditions $\xi_{ij}(0) = 0$ and $\dot{\xi}_{ij}(0) = v$. The collision is complete at time t_c when $\dot{\xi}_{ij}(t_c) = 0$ [6].

Of course, for a pairwise collision the final velocity as obtained from Eq. (1) must coincide with the final velocity as obtained from integrating Newton's equation of motion. Therefore, the solution $\dot{\xi}_{ij}(t_c)$ of Eq. (9) allows to relate the coefficient of restitution ε to the parameters k and γ of the force law, Eq. (7), via

$$\varepsilon = -\frac{\dot{\xi}(t_c)}{v}. \tag{10}$$

Straightforward calculation [6] yields for the duration of the collision

$$t_c = \begin{cases} \frac{1}{\omega}\left(\pi - \arctan\frac{2\beta\omega}{\omega^2-\beta^2}\right) & \text{for } \beta < \frac{\omega_0}{\sqrt{2}}, \\ -\frac{1}{\omega}\arctan\frac{2\beta\omega}{\omega^2-\beta^2} & \text{for } \beta > \frac{\omega_0}{\sqrt{2}}, \end{cases} \tag{11}$$

with

$$\omega_0^2 \equiv \frac{k}{m^{\text{eff}}}; \quad \beta \equiv \frac{\gamma}{2m^{\text{eff}}}; \quad \omega \equiv \sqrt{\omega_0^2 - \beta^2}. \tag{12}$$

Note that because of $\arctan(ix) = i\,\text{arctanh}(x)$ (where $i^2 = -1$ is the imaginary unit) the second branch of Eq. (11) holds true even for $\beta > \omega_0$ where ω becomes an imaginary number.

For the coefficient of restitution we obtain

$$\varepsilon = \begin{cases} \exp\left[-\frac{\beta}{\omega}\left(\pi - \arctan\frac{2\beta\omega}{\omega^2-\beta^2}\right)\right] & \text{for } \beta < \frac{\omega_0}{\sqrt{2}}, \\ \exp\left[\frac{\beta}{\omega}\arctan\frac{2\beta\omega}{\omega^2-\beta^2}\right] & \text{for } \beta \in \left[\frac{\omega_0}{\sqrt{2}},\omega_0\right], \\ \exp\left[-\frac{\beta}{\Omega}\ln\frac{\beta+\Omega}{\beta-\Omega}\right] & \text{for } \beta > \omega_0, \end{cases} \tag{13}$$

where $\Omega \equiv \sqrt{\beta^2 - \omega_o^2}$. Note that ε depends on the parameters of the force and the effective mass m^{eff} of the colliding particles; that is, $\varepsilon = \varepsilon(k,\gamma,m^{\text{eff}})$. Thus, ε may not be considered as a pure material constant.

III. SIMULTANEOUS CONTACTS

A. Equations of motion

The ICM fails if we take into account the finite duration of the collisions. In this case, it may happen that the collision of the particles (process b) starts yet before the collision of the lower particle with the floor (process a) has terminated. In this case we have a three-particle interaction of the floor and both balls which cannot be resolved using the concept of the coefficient of restitution. In this case, the final velocity of the upper particle must be determined by integrating Newton's equation of motion for the three-particle system which requires the detailed knowledge of the interaction forces. Consequently, we have to solve the set of Newton's equations

$$\begin{aligned} m_1\ddot{z}_1 + m_1 g + F_{12} - F_{01} &= 0, \\ m_2\ddot{z}_2 + m_2 g - F_{12} &= 0, \end{aligned} \tag{14}$$

where F_{ij} is the model-specific interaction law between particles i and j and the floor is considered as particle 0 (with $m_0 \to \infty$).

The failure of the simplifying ICM was discussed in, e.g., [7], and also in the context of the closely related problem of Newton's cradle. A simple analysis reveals immediately that the textbook-like explanation using isolated collisions is insufficient [8]. Instead, the details of the interaction force must

be taken into account. The explanation of Newton's cradle is far from being simple and there is an intensive and controversial discussion about this seemingly simple classroom experiment (see, e.g., [9,10] or the discussion started with [11]).

The necessity of considering the details of the interaction force becomes obvious immediately when considering colliding rods instead of spheres [12–15]. In fact, the investigation of longitudinal waves in colliding bodies and the corresponding duration of the collision is a classical problem of mechanics, investigated by some of the most eminent scientists, such as Poisson [16], Boltzmann [17], and other important scientists [18–20].

B. Comparison with the ICM

In Sec. II B we conclude the coefficient of restitution from the interaction force. Using this result, we can compute the final relative velocity v_r' by means of Eq. (4), employing the assumption of independent collisions. Alternatively we can obtain v_r' by solving the set of equations (14) numerically. The latter approach does not require any assumption on the sequence of the collisions. We will see that both results may deviate considerably according to rather complex dynamics of the system.

In order to compare both results by means of Eq. (13) we map the constants of the force law to the coefficient of restitution $(k,\gamma,m^{\text{eff}}) \leftrightarrow \varepsilon$.

We assume that the collisions between the lower sphere and the floor ($ij = 01$) and between the spheres ($ij = 12$) take place at the same coefficient of restitution. Since the effective mass enters Eq. (13), for given material stiffness, $k = \text{const.}$, Eq. (13) then provides a relation between ε and γ_{ij}; thus, we can determine γ_{ij} by specifying ε as a control parameter of the problem.

The latter assumption implies the somewhat unphysical fact that the lower side of the large sphere (where it contacts the floor) is characterized by a larger dissipative constant $\gamma_{01} \neq \gamma_{12}$ than its upper side (where it contacts the smaller sphere). We will justify this assumption in Appendix C where we show that the perhaps more plausible assumption $\gamma_{01} = \gamma_{12}$, implying $\varepsilon_{01} \neq \varepsilon_{12}$, leads to qualitatively identical results.

IV. BASKETBALL–TENNIS BALL PROBLEM

A. Collision sequence

Let us assume two vertically aligned balls (the basketball–tennis ball problem) as sketched in Fig. 1. We integrate Newton's equations of motion, Eqs. (14), for this system numerically and obtain the forces between the bottom and the lower sphere and between both spheres, see Fig. 2.

For time $t_{01}^{(b)} \leqslant t \leqslant t_{01}^{(e)}$ the lower particle is in contact with the floor as indicated by the force $F_{01} \neq 0$. During this interval the balls are in contact repeatedly, starting at time (first contact) $t_{12}^{(b)}$ and ending (last contact) at time $t_{12}^{(e)}$ as indicated by $F_{12} \neq 0$. An interesting detail is the discontinuity of F_{01} at $t = t_{01}^{(b)}$ which is a consequence of the force law, Eq. (7): At the instant of the contact where $\xi_{01} \to 0$, the elastically restoring term, $k\xi_{01}$, vanishes whereas the (repulsive) dissipative term, $\gamma\dot{\xi}_{01}$, has a finite value as soon as the particles get into contact.

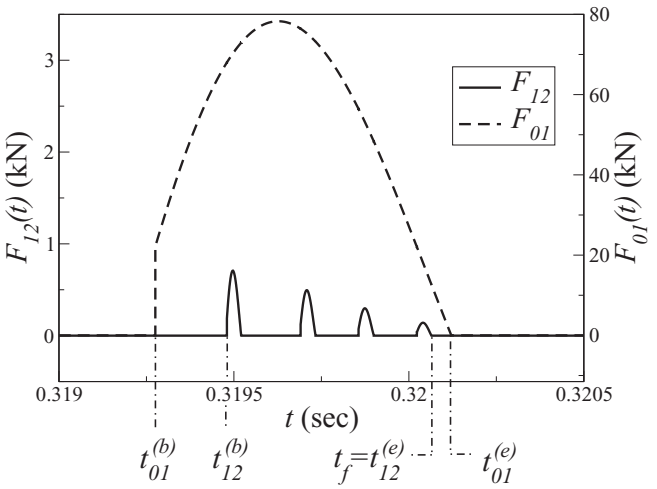

FIG. 2. Forces F_{01} and F_{12} obtained from solving Eqs. (14). During the contact between the lower particle and the floor there occur multiple contacts between the spheres (full line). For discussion see the text. Parameters: $R_1 = 10$ cm, $R_2 = 1$ cm, $\Delta h = 0.1$ mm, $z_1^{(0)} = 0.6$ m, $k = 5 \times 10^7$ N/m, and $\varepsilon = 0.7$.

The existence of multiple collisions shown in Fig. 2 shows that the ICM described in Sec. II fails for the chosen set of parameters which provokes mainly two questions:

(1) How many contacts between the spheres occur and how does their number depend on the system parameters (Δh, R_1, R_2, γ_{ij}, or ε)?

(2) If multiple collisions take place, when does the collision sequence terminate?

Depending on the system parameters we may obtain $t_{12}^{(e)} \leqslant t_{01}^{(e)}$ or $t_{12}^{(e)} > t_{01}^{(e)}$; therefore, the second question must be answered by a definition: The collision-sequence terminates at time $t = t_f$ (see Fig. 2) when the last contact between the spheres ceases, before the large sphere collides with the floor for the second time.

To answer the first question we refer to Fig. 3, which illustrates the sequence of collisions in dependence of the coefficient of restitution ε for fixed Δh and R_1/R_2. The value of ε was adjusted by varying γ according to Eq. (13) while keeping $k = 5 \times 10^7$N/m invariant. Figure 3 should be read horizontally (for fixed value of ε): Each black or gray line marks time intervals when the particles are in contact. For elastic balls, $\varepsilon = 1$, and for the chosen parameters there occur 3 collisions. For sufficiently large Δh, this number may be unity; that is, the independent-collisions condition is fulfilled (see below). Keeping Δh, k, and the radii R_1 and R_2 constant and decreasing ε, the number of contacts increases. This is due to the fact that the relative velocity of the balls decreases because of inelastic collisions and, thus, the intervals of free flight become shorter while the duration of the contacts depends only weakly on the value of the inelasticity. For yet smaller ε the relative velocity after the kth contact may be small enough such that the lower ball catches up with the upper because of its upward acceleration due to its contact with the floor. This effect makes some free-flight intervals vanish for decreasing ε and, thus, reduces the number of contacts. Summarizing, for each set of parameters $\{\Delta h, R_1, R_2, k\}$ the number of collisions as a function of ε is a function with a single maximum.

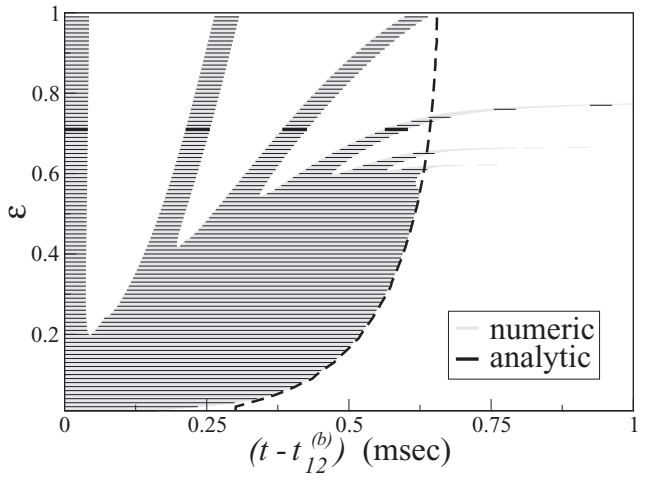

FIG. 3. Sequence of collisions for varying coefficient of restitution. The dashed line shows the end of the contact between the lower sphere and the floor, $t_{01}^{(e)}$. The thick line corresponds to the force drawn in Fig. 2 ($R_1 = 10$ cm, $R_2 = 1$ cm, $\Delta h = 0.1$ mm, $z_1^{(0)} = 0.6$ m, and $k = 5 \times 10^7$ N/m).

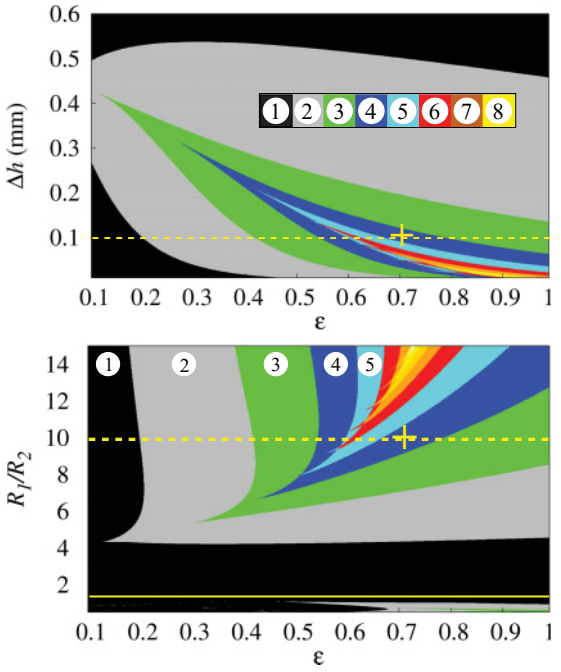

FIG. 4. (Color online) Number of contacts between the spheres as a function of ε and Δh (top) and ε and R_1/R_2 (bottom). The dashed lines show the value of Δh and R_1/R_2 used in Fig. 3; the + symbol shows the parameters used in Fig. 2. The solid line in the lower panel indicates $R_1/R_2 = 1$ [parameters: $k = 5 \times 10^7$ N/m, $R_1 = 10$ cm, and $R_2 = 1$ cm (top); and $k = 5 \times 10^7$ N/m, $R_2 = 1$ cm, and $\Delta h = 0.1$ mm (bottom)].

For the force law Eq. (7) the basketball–tennis ball problem may be solved analytically by a piecewise procedure, see Appendix A. To check against numerical errors, the horizontal gray lines (in between the black lines) show the same information as the result of an analytical theory (black lines) which agrees perfectly with the numerical data.

There is an interesting case when the final velocity of the lower ball after losing contact with the floor is only slightly larger than the velocity of the upper ball after the previous collision. Since both balls move only under the action of gravity, the balls may collide an ultimate time even after the contact between the lower ball and the floor has already finished. These events may be seen in Fig. 3 as narrow spikes at $\varepsilon \approx 0.78$, $\varepsilon \approx 0.67$, etc.

The number of contacts of the spheres as a function of ε and the initial distance Δh is shown in more detail in Figure 4 (top). As explained above for each value of ε there is an interval for Δh which maximizes the number of contacts.

For the interaction force, Eq. (7), the ratio $t_{c,01}/t_{c,12}$ of the contact duration of the collision lower sphere/ground $t_{c,01}$ and the contact duration of the collision lower sphere/upper sphere $t_{c,12}$ increases with m_1/m_2 (or R_1/R_2, respectively). Consequently, the number of contacts increases with R_1/R_2, shown in Fig. 4 (bottom). On the other hand, increasing R_1/R_2 also increases the initial relative velocity between the two spheres and with that the intervals of free flight, which in turn reduces the possible number of contacts. While the effect explained first is dominating, the interplay of both effects explains the rather complex behavior shown in the bottom panel of Fig. 4.

From Figs. 3 and 4 we see that for a vast range of parameters the true collision scenario as obtained from the integration of Newton's equations of motion deviates drastically from the independent-collision scenario outlined in Sec. II.

B. Effective coefficient of restitution

By solving Newton's equation, we can compute the final relative velocity $v_r' = v_2(t_f) - v_1(t_f)$ which corresponds to Eq. (4) obtained from the ICM. To compare both results, we compute v_r' by integrating Eqs. (14) using the interaction force Eq. (7) for a certain set of parameters $\{\Delta h, m_1, m_2, k\}$ and a specified $\varepsilon = \varepsilon_{\text{spec}}$ [which in turn determines γ via Eq. (13)]. Then, by inverting Eq. (4) we determine the coefficient of restitution $\varepsilon = \varepsilon_{\text{eff}}$ which would yield the same final relative velocity for the ICM. If $\varepsilon_{\text{eff}}/\varepsilon_{\text{spec}} \approx 1$, both models yield the same result; that is, the ICM is an acceptable approximation. Otherwise, the ICM fails.

Consider the dependence of $\varepsilon_{\text{eff}}/\varepsilon_{\text{spec}}$ on the initial distance Δh. For large Δh the lower sphere leaves the floor before it contacts the upper one; that is, the ICM holds true. Figure 5 (top) shows that $\varepsilon_{\text{eff}}/\varepsilon_{\text{spec}} \to 1$ with increasing Δh. Moreover, as expected for $\varepsilon_{\text{eff}}/\varepsilon_{\text{spec}} \to 1$ there is only one contact which is a necessary (but not sufficient) precondition for independent collisions. Figure 5 (bottom) is a magnification of the range of small Δh. As discussed before, the number of contacts as a function of Δh has a maximum. The oscillations in the number of contacts as a function of Δh for very small Δh correspond to the spikes shown in Fig. 3 where the lower sphere catches up with the upper after the lower sphere has already left the ground.

Similarly, Fig. 6 shows $\varepsilon_{\text{eff}}/\varepsilon_{\text{spec}}$ as a function of R_1/R_2. Since increasing R_1/R_2 increases the number of contacts, $\varepsilon_{\text{eff}}/\varepsilon_{\text{spec}}$ decreases and thus, as expected, the ICM invalidates with increasing R_1/R_2.

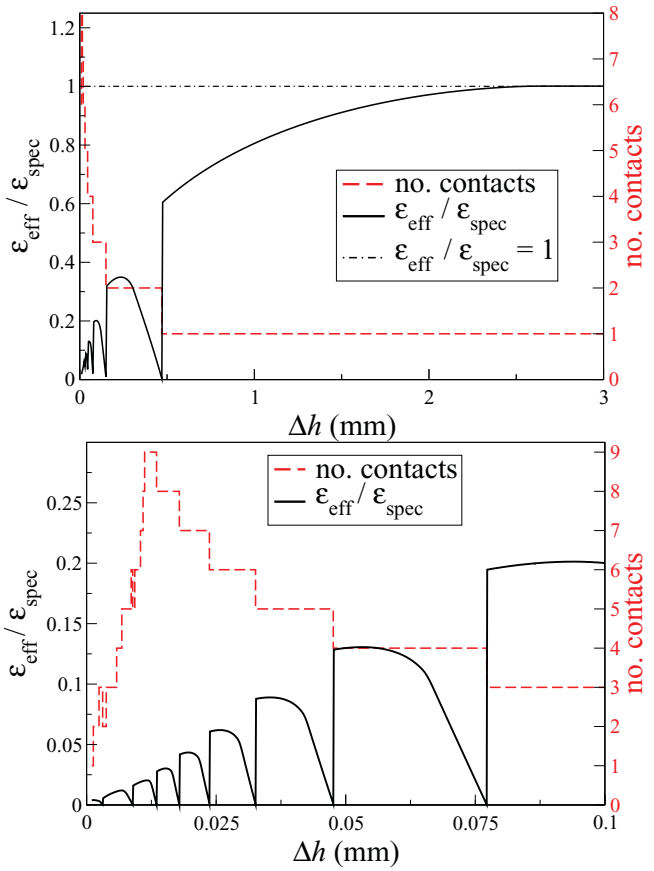

FIG. 5. (Color online) $\varepsilon_{\text{eff}}/\varepsilon_{\text{spec}}$ as a function of Δh and the corresponding number of contacts (right axis, top). The bottom figure shows a magnification of the small Δh range. Parameters: $R_1 = 10\,\text{cm}$, $R_2 = 1\,\text{cm}$, $k = 5 \times 10^7\,\text{N/m}$, and $\varepsilon_{\text{spec}} = 0.9$.

For most values of the parameter space we observe multiple collisions leading to additional dissipation ($\varepsilon_{\text{eff}}/\varepsilon_{\text{spec}} < 1$). On the other hand, having only one contact does not necessarily imply independent collisions. For $R_1 \approx R_2$ because of similar particle masses and similar durations of the contact between the upper sphere and the lower sphere and between the lower sphere and the floor, coupling becomes important in the equations of motion Eq. (14). The complex dynamics of the (fully) coupled system may lead to additional or reduced dissipation as compared with the ICM. The inset in Fig. 6 shows the small interval of R_1/R_2 where $\varepsilon_{\text{eff}}/\varepsilon_{\text{spec}} > 1$ (reduced dissipation). Only in this small region we find $\varepsilon_{\text{eff}} > \varepsilon_{\text{spec}}$.

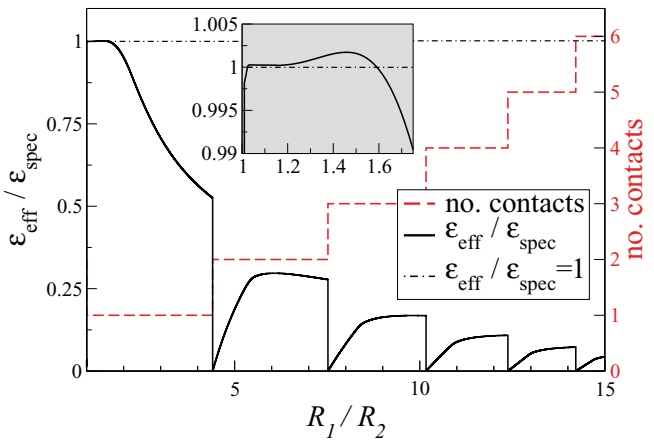

FIG. 6. (Color online) $\varepsilon_{\text{eff}}/\varepsilon_{\text{spec}}$ as a function of R_1/R_2 (with $R_2 =$ 1cm) and the corresponding number of contacts (right axis). Further parameters: $k = 5 \times 10^7\,\text{N/m}$, $\varepsilon_{\text{spec}} = 0.8$, and $\Delta h = 0.1\,\text{mm}$.

V. CONCLUSION

We considered the motion of two vertically aligned spheres which are released to collide with the floor under the action of gravity. For the analysis of the dynamics of this textbook problem (basketball–tennis ball problem) we used two complementary methods. First we described the system exploiting the *independent-collisions model* (ICM) which assumes instantaneous collisions between the spheres and between the lower sphere and the floor. The collisions are described by a single number, the coefficient of restitution, ε, and the duration of the collisions is neglected. Second, we described the dynamics by analytically and numerically solving Newton's equation of motion. Here the collisions are characterized by an interaction force law, $F(\xi,\dot{\xi})$. For the case of the linear-dashpot model used here, the force is a function of the elastic and dissipative parameters k and γ. Since there is a direct relation between ε and $\{k,\gamma\}$, we can compare the results of the ICM and the solution of Newton's equations.

We specify two characteristics of the process, (a) the final relative velocity, v', between the spheres and (b) the number of collisions between the spheres during the process. If the approaches were equivalent, we should obtain equivalent results for (a) and (b).

Obviously, in case of the ICM there is only one collision between the spheres and the final result for v' is the solution of a textbook problem, Eq. (4). In the article we show that Newton's equations yield a different scenario, including multiple collisions, and the ICM is only valid in a certain limit; that is, the ICM fails for a wide range of parameters.

To quantify the deviations, we solve Newton's equations with parameters k and γ that correspond to a certain specified coefficient of restitution $\varepsilon = \varepsilon_{\text{spec}}$. Then we compare this value with the *effective* coefficient of restitution, ε_{eff}, obtained from the final relative velocity as obtained from Newton's equation. The value $\varepsilon_{\text{eff}}/\varepsilon_{\text{spec}} = 1$ would indicate that both models agree. Our results reveal, however, a dramatic deviation from this ideal behavior. In Figs. 5 and 6 we see that in contradiction to the ICM, the ratio $\varepsilon_{\text{eff}}/\varepsilon_{\text{spec}}$ may adopt any value from almost zero up to slightly larger than one; that is, the ICM fails dramatically.

While our subject, the basketball–tennis ball problem, is only a cute but relatively unimportant toy problem, our results may have serious consequences for numerical simulation techniques of granular many-particle problems. There exist two established simulation techniques for the simulation of granular systems, molecular dynamics (MD) and event-driven molecular dynamics (EMD). While MD solves Newton's equations of motion for all N particles constituting the granular system, and thus solves a system of $3N$ (without rotation) coupled, strongly nonlinear differential equations,

EMD describes the dynamics of the N-particle system as a sequence of pairwise collisions. The latter approach allows for a great speedup of the numerical simulation since instead of solving computer-time-intensive solutions of differential equations, we only have to compute postcollisional velocities from the precollisional ones, as a function of the coefficient of restitution for each pair of colliding particles, $\{\vec{v}_i,\vec{v}_j,\varepsilon\} \to \{\vec{v}_i',\vec{v}_j'\}$, via a simple propagation function. In between the collisions the particles follow simple ballistic trajectories.

It is obvious that EMD allows for very efficient simulations as compared with MD, in particular for large $N \sim 10^6 \ldots 10^8$; however, this speedup comes at the price of the assumption of independent collisions, that is, EMD assumes instantaneous collisions neglecting the duration of the collisions. While this assumption may be justified in a granular gas where the mean free flight time is large as compared to the typical duration of collisions, it fails for dense systems. Our simple one-dimensional, 3-particle system shows that the failure may be dramatic.

For the analytical calculations presented in this article we made two major assumptions whose justification might not be obvious beforehand: First we assumed a linear-dashpot force, Eq. (7), for the interaction of viscoelastic spheres. This force allows for a simple mapping of the constants k and ε to the coefficient of restitution which is, moreover, a constant in this case. Of course, the interaction of spheres is described by a (modified) Hertz law which leads to an impact velocity dependent ε. We could perform the entire calculation presented here also for the Hertz law, however, at a *much* larger mathematical effort (see [21] for a similar calculation). We prefer here the simplified force and demonstrate in Appendix B that the Hertz law leads to qualitatively identical results.

The second simplification concerns the assumption of a universal coefficient of restitution for the description of the collisions between the particles and between the lower particle and the floor. Since the effective mass enters the mapping between the force constants and ε, the assumption of a universal ε implies that the lower sphere is characterized by a certain set of parameters $\{k,\gamma\}$ when colliding with the floor, but by a different set of parameters when colliding with the upper sphere. The alternative assumption of invariant material parameters is, perhaps, more plausible but leads then to different values of the coefficient of restitution for particle-particle and particle-floor collisions. While these alternative assumptions lead, of course, to different results, in Appendix C we demonstrate that the qualitative properties of the dynamics are the same for both assumptions.

APPENDIX A: ANALYTICAL DESCRIPTION

For an approximative analytical description, we assume that the motion of the large ball is not affected by the small ball. This adiabatic approximation becomes exact for $R_1 \gg R_2$, and Eqs. (14) decouple and may be solved piecewise. We obtain four different types of collective motion:

Type A. The balls are isolated from one another and from the floor. Here the particles move along ballistic trajectories

$$z_{1,\mathrm{free}}(t) = -gt^2/2 + v_1^{(k)}t + z_1^{(k)}\,, \tag{A1}$$

$$z_{2,\mathrm{free}}(t) = -gt^2/2 + v_2^{(k)}t + z_2^{(k)}\,. \tag{A2}$$

In our notation $v_i^{(k)}$ and $z_i^{(k)}$ stand for the positions and velocities of the particles at the instant when the system enters a type of motion for the kth time; that is, they are initial conditions of the piecewise analytical solution.

Type B. The lower ball is in contact with the floor while the upper one moves freely. Here the upper sphere moves along a ballistic trajectory, $z_{2,\mathrm{free}}(t)$, while the lower one moves according to a damped harmonic oscillator,

$$m_1\ddot{z}_1 = -m_1 g + k_1(R_1 - z_1) - \gamma_1\dot{z}_1 \tag{A3}$$

with the solution

$$z_{1,\mathrm{ground}}(t) = A\cos[\omega t + p]e^{-\lambda t} + z_{1,\mathrm{inh}}\,, \tag{A4}$$

where

$$p = \arctan\left[\frac{\lambda\left(z_1^{(k)} - z_{1,\mathrm{inh}}\right) + v_1^{(k)}}{(z_{1,\mathrm{inh}} - z_1^{(k)})\omega}\right];$$

$$A = \frac{z_1^{(k)} - z_{1,\mathrm{inh}}}{\cos(p)}; \quad z_{1,\mathrm{inh}} = \frac{k_1R_1 - m_1g}{k_1};$$

$$\lambda = \frac{\gamma_1}{2m_1}; \quad \omega = \sqrt{\omega_0^2 - \lambda^2}; \quad \omega_0 = \sqrt{k_1/m_1}\,.$$

Type C. The balls are in contact and the lower ball contacts the floor. Here the lower sphere moves due to Eq. (A4), disregarding the force resulting from the contact with the upper sphere (adiabatic approximation). The latter moves like a damped harmonic oscillator in the presence of gravity, additionally driven by the motion $z_{1,\mathrm{ground}}(t)$ of the lower sphere:

$$m_2\ddot{z}_2 = -m_2 g + k_2[R_1 + R_2 - (z_2 - z_{1,\mathrm{ground}})] - \gamma_2(\dot{z}_2 - \dot{z}_{1,\mathrm{ground}}). \tag{A5}$$

The solution $z_{2,\mathrm{ground}}(t)$ of Eq. (A5) is straightforward and similar to Eq. (A4) but since it is rather lengthy it is not given here.

Type D. The balls are in contact with each other but not with the floor. Here the lower sphere follows a ballistic trajectory disregarding the force resulting from the contact with the upper one (adiabatic approximation) and the upper sphere moves as described in type C but now driven by the motion $z_{1,\mathrm{free}}(t)$ of the lower sphere:

$$m_2\ddot{z}_2 = -m_2 g + k_2[R_1 + R_2 - (z_2 - z_{1,\mathrm{free}})] - \gamma_2(\dot{z}_2 - \dot{z}_{1,\mathrm{free}})\,. \tag{A6}$$

Again we do not provide the lengthy but straightforward solution $z_{2,\mathrm{air}}(t)$ of Eq. (A6) here.

We keep in mind that balls i and j (with $i = 0$ representing the floor) are in contact if the mutual compression ξ_{ij} is positive and the interaction force F_{ij} is repulsive. Then we obtain the analytical solution of the problem, $z_1(t)$ and $z_2(t)$, from combining the analytical solutions of the cases A–D by means of the following scheme:

(1) Type A motion until the lower sphere touches the floor at T_{bcl} where $[\xi_{01}(T_{\mathrm{bcl}}) > 0] \wedge [F_{01}(T_{\mathrm{bcl}}) > 0]$.

(2) Type B motion until the spheres contact each other at $T_{\rm bcu}$ where $[\xi_{12}(T_{\rm bcu}) > 0] \wedge [F_{12}(T_{\rm bcu}) > 0]$.

(3) Type C motion until the contact between the spheres breaks at $T_{\rm ecu}$ where $F_{12}(T_{\rm ecu}) \leqslant 0$.

(4) Repeat steps 2 and 3 until the lower sphere leaves the floor at $T_{\rm ecl}$ where $F_{01}(T_{\rm ecl}) \leqslant 0$:

If $T_{\rm bcu} > T_{\rm ecl} \rightarrow$ type B motion until $T_{\rm ecl}$.

If $T_{\rm ecu} > T_{\rm ecl} \rightarrow$ type C motion until $T_{\rm ecl}$ and then type D motion until the spheres separate at $T_{\rm ecu}$ where $F_{12}(T_{\rm ecu}) \leqslant 0$.

(5) Type A motion until

(a) the lower sphere contacts the floor for the second time at $T_{\rm bcl}$ where $[\xi_{01}(T_{\rm bcl}) > 0] \wedge [F_{01}(T_{\rm bcl}) > 0]$, or

(b) the spheres touch each other again at $T_{\rm bcu}$ where $[\xi_{12}(T_{\rm bcu}) > 0] \wedge [F_{12}(T_{\rm bcu}) > 0]$.

In the first case the collision sequence has terminated. In the second case: type D motion until the spheres separate at $T_{\rm ecu}$ where $F_{12}(T_{\rm ecu}) \leqslant 0$ or until the lower sphere contacts the ground at $T_{\rm bcl}$ where $[\xi_{01}(T_{\rm bcl}) > 0] \wedge [F_{01}(T_{\rm bcl}) > 0]$.

The described procedure seems to be circumstantial but it provides an exact analytical solution of the problem in adiabatic approximation.

APPENDIX B: VALIDITY OF THE SIMPLIFIED FORCE MODEL

The purpose of this Appendix is to demonstrate that the analytical and numerical results presented in Sec. IV are more than just artifacts of the simplified interaction force Eq. (7). The reason for the deviation of the *effective* coefficient of restitution from the *specified* coefficient shown in Figs. 5 and 6 is the described multiple collisions arising from the finite duration of the collisions. Therefore, here we show that multiple collisions also appear for the much more realistic interaction force Eq. (B1). To this end we reproduce Fig. 3 where the time intervals of particle contacts are shown in dependence on the (specified) coefficient of restitution.

1. Viscoelastic spheres

The force law, Eq. (7), is convenient as it leads to a coefficient of restitution, Eq. (13), in an elementary way. However, this force law is a strong simplification. Perhaps the simplest particle interaction model which is not in conflict with basic mechanics of materials is the contact of viscoelastic spheres, i and j [5], given by

$$\frac{F(\xi_{ij},\dot{\xi}_{ij})}{m_{ij}^{\rm eff}} = \min\left[0, -k\xi_{ij}^{3/2} - \gamma\sqrt{\xi_{ij}}\dot{\xi}_{ij}\right], \qquad \text{(B1)}$$

with

$$\rho \equiv \frac{2Y\sqrt{R_{ij}^{\rm eff}}}{3(1-\nu^2)}, \quad k \equiv \frac{\rho}{m_{ij}^{\rm eff}}, \quad \gamma \equiv \frac{3}{2}\frac{\rho A}{m_{ij}^{\rm eff}}, \qquad \text{(B2)}$$

the Young modulus Y, Poisson's ratio ν, the effective radius $R_{ij}^{\rm eff} = R_i R_j/(R_i + R_j)$, and the effective mass $m_{ij}^{\rm eff} = m_i m_j/(m_i + m_j)$. Again we use the mutual compression and the compression rate to describe the contact dynamics [see Eq. (8)]. The dissipative constant A is a function of the material viscosity; see [5] for details. For *elastic* spheres, $A = 0$, we recover the classical Hertz contact force [22].

A necessary prerequisite for deriving Hertz's law of contact and its generalization to viscoelastic spheres, Eq. (B1), is the assumption of small particle deformation; that is, the interaction force causes only local displacements in the region of the contact area. Moreover, the impact rate must be small as compared to the speed of sound to allow for a quasistatic approximation, see [5]. More complex deformations including surface waves and oscillations, e.g., [23], are not considered here. Such oscillations may also give rise to multiple collisions between particles and yet more complicated particle-particle interaction.

The relation between the coefficient of restitution and the parameters of the force law, corresponding to Eq. (13), may also be obtained for the case of viscoelastic spheres. The calculation is cumbersome [21,24] (a simplified version is based on a dimension analysis [25]); here we present only the result:

$$\varepsilon(v) = \sum_{k=0}^{\infty} h_k \beta^{k/2} v^{k/10}, \qquad \text{(B3)}$$

with the initial conditions $\xi_{ij}(0) = 0$ and $\dot{\xi}_{ij}(0) = v$ and with $\beta \equiv \gamma k^{-3/5}$ and the pure numbers $h_0 = 1$, $h_1 = 0$, $h_2 = -1.153$, $h_3 = 0$, $h_4 = 0.798$, $h_5 = 0.267$, ... (see [21] for the numerical values h_k). Note that in contrast to the previous case, Eq. (13), here the coefficient of restitution depends on the impact velocity v.

2. Basketball–tennis ball problem for viscoelastic balls

Just as in Sec. IV, we use the coefficient of restitution ε to characterize the system's dissipative properties, due to the dissipative constant A in the force law, Eq. (B1). We proceed along the lines of Sec. IV A: We specify ε, the Young modulus Y, Poisson's ratio ν, and the effective radius $R_{ij}^{\rm eff}$ and mass $m_{ij}^{\rm eff}$, and solve Eq. (B3) numerically for the dissipative parameter A. Additionally, we specify the initial velocity $v_{\rm in} = 3$ m/s since for the viscoelastic force law the coefficient of restitution depends on the impact rate. As in Sec. IV, the assumption of a universal value of the coefficient of restitution to describe both particle-particle and particle-floor contact results in the rather artificial fact that the spheres cannot consist of the same material. This assumption is necessary to use the quite descriptive quantity ε as a control parameter. In Appendix C we will release this assumption and show that it does not qualitatively change the system's behavior.

Figure 7 shows the sequence of collisions, corresponding to Fig. 3 for the linear-dashpot force. The figures reveal the same structure of the collision scenario; that is, the viscoelastic force, Eq. (B1), leads to qualitatively the same results as the linear-dashpot model and, thus, justifies application of the simplified force Eq. (7) in Sec. IV.

Using identical system geometry and particle masses, a quantitative comparison between the simplified interaction force Eq. (7) and the viscoelastic model Eq. (B1) would require the matching of the elastic constants k in Eq. (7) and ρ in Eq. (B1). As there is no straight, general rule for matching, a fair quantitative comparison is impossible. Nevertheless we attempt a quantitative comparison by matching the elastic constant k and the Young modulus Y, such that to achieve the defined overlap $(R_1 + R_2)/10$ the same force is needed in both

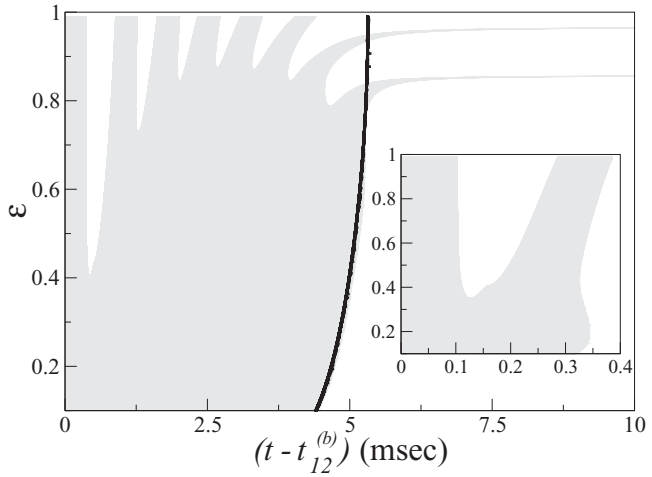

FIG. 7. Same as Fig. 3 but for viscoelastic spheres. Parameters: $R_1 = 10\,\mathrm{cm}$, $R_2 = 0.25\,\mathrm{cm}$, $\Delta h = 0.1\,\mathrm{mm}$, $Y = 5 \times 10^7\,\mathrm{N/m^2}$, and $\nu = 0.45$. The black line shows the end of the contact between the lower sphere and the floor for each ε. The inset shows the result using the system geometry and particle masses from Fig. 3. The Young modulus $Y = 6 \times 10^9\,\mathrm{N/m^2}$ was matched to Fig. 3 as described in the text.

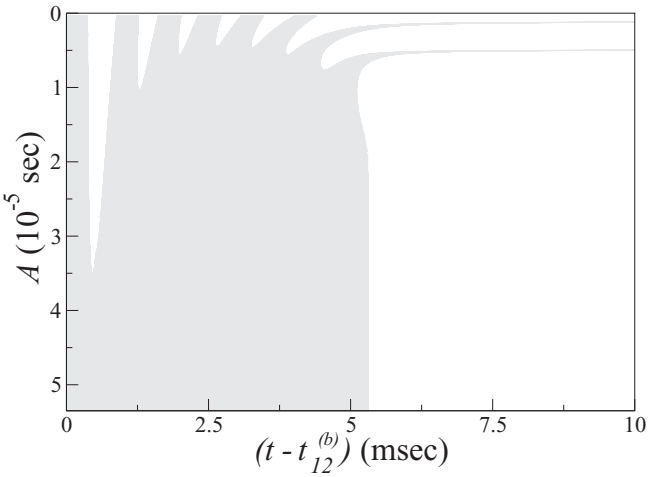

FIG. 8. Same as Fig. 7 but for particles made from the same material, characterized by the dissipative material parameter A. Parameters: $R_1 = 10\,\mathrm{cm}$, $R_2 = 0.25\,\mathrm{cm}$, $\Delta h = 0.1\,\mathrm{mm}$, $Y = 5 \times 10^7\,\mathrm{N/m^2}$, and $\nu = 0.45$).

models. By showing the collision sequence for viscoelastic spheres, the inset in Fig. 7 displays the result. Even for a system geometry identical to the one used in Fig. 3 and the matched Young modulus, we observe multiple collisions, i.e., a deviation from the ICM.

APPENDIX C: VALIDITY OF THE ASSUMPTION OF A UNIVERSAL COEFFICIENT OF RESTITUTION

For the calculations we assumed that the collisions between the lower sphere and the floor and between the spheres occur via the same coefficient of restitution ε which allows us to consider ε as a control parameter. This assumption, however, implies also different dissipative constants for the contacts.

In this Appendix we reproduce Fig. 7 once again with the complementary assumption of identical material parameters, which implies in its turn different coefficients of restitution ε_{01} for the particle-floor and ε_{12} for the particle-particle contact, see Fig. 8. Thus, we can no longer use ε as characteristic value. Instead, to characterize the interaction we use the dissipative material parameter A which enters the force law, Eq. (B1).

The sequence of collisions shown in Fig. 3 has the same structure as for the assumption of a universal coefficient of restitution with only minor quantitative differences. Still there occur multiple collisions and consequently the effects described in Sec. IV persist. Hence the assumption of a universal coefficient of restitution is justified.

[1] W. G. Harter, Am. J. Phys. **39**, 656 (1971).
[2] W. R. Mellen, Phys. Teach. **33**, 56 (1995).
[3] P. Patrício, Am. J. Phys. **72**, 1488 (2004).
[4] J. D. Kerwin, Am. J. Phys. **40**, 1152 (1972).
[5] N. V. Brilliantov, F. Spahn, J.-M. Hertzsch, and T. Pöschel, Phys. Rev. E **53**, 5382 (1996).
[6] T. Schwager and T. Pöschel, Granular Matter **9**, 465 (2007).
[7] R. Cross, Am. J. Phys. **75**, 1009 (2007).
[8] J. V. Kline, Am. J. Phys. **28**, 102 (1960).
[9] S. Chapman, Am. J. Phys. **28**, 705 (1960).
[10] E. J. Hinch and S. Saint-Jean, Proc. R. Soc. London A **455**, 3201 (1999).
[11] F. Herrmann and P. Schmälzle, Am. J. Phys. **49**, 761 (1981).
[12] D. Auerbach, Am. J. Phys. **62**, 522 (1994).
[13] R. Cross, Am. J. Phys. **76**, 908 (2008).
[14] H. Maecker, Naturwissenschaften **40**, 521 (1953).
[15] C. C. Fu and B. Paul, Int. J. Numer. Methods Eng. **2**, 363 (1970).
[16] S. D. Poisson, *Traité de Mécanique* (Bachelier, Paris, 1833).
[17] L. Boltzmann, *Wissenschaftliche Abhandlungen*, edited by Fritz Hasenöhrl (AMS Bookstore, 2001).
[18] W. Voigt, Ann. Phys. **351**, 657 (1915).
[19] H. R. Schneebeli, Ann. Phys. **219**, 239 (1871).
[20] M. Hamburger, Ann. Phys. **264**, 653 (1886).
[21] T. Schwager and T. Pöschel, Phys. Rev. E **78**, 051304 (2008).
[22] H. Hertz, J. Reine Angew. Math. **92**, 156 (1882).
[23] R. Cross, Am. J. Phys. **67**, 222 (1999).
[24] T. Schwager and T. Pöschel, Phys. Rev. E **57**, 650 (1998).
[25] R. Ramírez, T. Pöschel, N. V. Brilliantov, and T. Schwager, Phys. Rev. E **60**, 4465 (1999).